

Gale A. Holmes,¹ Richard C. Peterson,¹ Donald L. Hunston,¹
Walter G. McDonough,¹ and Carol L. Schutte¹

The Effect of Nonlinear Viscoelasticity on Interfacial Shear Strength Measurements

REFERENCE: Holmes, G. A., Peterson, R. C., Hunston, D. L., McDonough, W. G., and Schutte, C. L., “**The Effect of Nonlinear Viscoelasticity on Interfacial Shear Strength Measurements,**” *Time Dependent and Nonlinear Effects in Polymers and Composites, ASTM STP 1357*, R. A. Schapery and C. T. Sun, Eds., American Society for Testing and Materials, West Conshohocken, PA, 2000, pp. 98-117.

ABSTRACT: Experimental evidence demonstrates that diglycidyl ether of bisphenol-A (DGEBA) / meta phenylenediamine (m-PDA) epoxy resin matrix used in the single fiber fragmentation tests exhibits nonlinear stress strain behavior in the region where E-glass fiber fracture occurs. In addition, strain hardening after the onset of yield is observed. Therefore, linear elastic shear-lag models and the Kelly-Tyson model are inappropriate for the determination of the interfacial shear strength for this epoxy resin system. Using a strain-dependent secant modulus in the Cox model, the calculated interfacial shear strength is shown to be relatively lower by at least 15 % than the value determined using a linear elastic modulus. This decrease is consistent with numerical simulations which show the linear elastic approximation over predicts the number of fragments in the fragmentation test. In addition, the value obtained by the strain-dependent secant modulus is approximately 300 % relatively higher than the value predicted by the Kelly-Tyson model.

KEYWORDS: single-fiber fragmentation test, viscoelasticity, nonlinear matrix behavior, strain-rate dependence, interfacial shear strength, epoxy resin, E-glass fiber, Cox Model, Kelly-Tyson model.

In most composite interface research, the strength and durability of the fiber-matrix interface are estimated by interfacial shear strength measurements. To a large extent, estimates of the fiber-matrix interfacial shear strength are based on unit composite micromechanics models and experimental data from single fiber fragmentation (SFF) tests. In the single fiber fragmentation test, a dogbone is made with a resin having a high extension-to-failure and a single fiber embedded down the axis of the dogbone. The sample is pulled in tension and stress is transmitted into the fiber through the fiber-matrix interface. Since the fiber has a lower strain to failure than the resin, the fiber breaks as the strain is increased. This process continues until the remaining fiber fragments are all less than a critical transfer length, l_c . The critical transfer length is the length below which the fragments are too short for sufficient load to be transmitted into them to cause failure. This point is termed saturation. The fragment lengths at saturation are measured and a micromechanics model is used to convert the average fragment length into a measure of the interface strength or stress transfer efficiency.

The fiber-matrix interfacial shear strength is a critical parameter since it directly affects off-axis properties in unidirectional composites and the shear strength of laminates. One of the central issues in predicting the long-term performance of a composite structure involves assessing the durability of the fiber-matrix interface. Although silane coupling agents are of-

¹ National Institute of Standards and Technology, Polymers Division, Gaithersburg, MD 20899

ten added to the fiber to enhance the durability of this interface, there is no reliable method to measure the effectiveness of these treatments. The matrix properties play a strong role in determining the interfacial shear strength and the matrix properties usually change dramatically with environmental exposure, via plasticization. Therefore, the integrity of the fiber-matrix interface cannot be assessed without properly accounting for the changes in the matrix properties. In addition, delayed fracture events have been shown to occur during the testing procedure at times greater than 10 min after the implementation of a step-strain increment. This behavior is inconsistent with elastic and elastic-perfectly plastic based micromechanics models and suggests the presence of a time dependent failure process. The latter observation parallels research on full composites that relates time dependent fracture of composites to nonelastic properties of the matrix. These results and observations suggest that a critical look at the influence of matrix properties on the shear stress transfer process in micromechanics models is needed.

Background & Approach

Research by Galiotis *et al.* [1] on polydiacetylene fiber embedded in an epoxy matrix has demonstrated that the fiber stress distribution in a SFF test specimen can be approximated by the “classical” shear lag model derived by Cox [2]. Galiotis [3] also notes that the constant shear stress condition across the fiber matrix interface is seldom achieved in polymer matrix composites. Hence, the Kelly-Tyson model [4-6], based on elastic-plastic analysis, for determining interfacial shear strength is seldom applicable to polymer matrix composites. In addition, experimental data on the DGEBA/m-PDA epoxy resin will be presented which demonstrates the inappropriateness of the constant shear stress approximation for this DGEBA/m-PDA resin system. Therefore, in this paper we will focus primarily on shear lag micromechanics models.

In developing the “classical” and “non-classical” shear lag models, researchers typically make simplifying assumptions about the shear-stress transfer process, the fiber-matrix interface, and the matrix material [7]. The common assumptions are as follows: (1) the matrix material is linear elastic, (2) a perfect bond exists between the fiber and the matrix, (3) the radius of the matrix, r_m , is unknown and typically assumed to be 1/2 the thickness of the test specimen, and (4) yielding of the matrix is not considered. In addition, as noted by Shioya *et al.* [88], these models make no assumption about the failure process occurring at the interface.

The “classical” shear lag models developed over the years [2,9-16] provide similar stress distribution profiles of the embedded fiber. However, these models violate the boundary conditions in the shear equation by predicting the maximum shear stress to be at the fiber ends. “Non-classical” shear lag models, developed recently by Whitney and Drzal [17], McCartney [18], and Nairn [19], overcome this violation. The shear stress profiles obtained from these “non-classical” models exhibit the appropriate zero shear stress at the fiber ends and fiber stress profiles similar to those predicted in the “classical” models. In addition, these models, along with a “classical” model developed by Amirbayat & Hearle [12-14] account for the radial pressure at the fiber-matrix interface that results from the difference in thermal expansion coefficients of the two materials. However, all of these models assume that the matrix material is linear elastic (the Kelly-Tyson model assumes elastic-perfectly plastic matrix behavior).

In applications that are strength and weight critical the matrix material, *e.g.*, tetraglycidyl-4,4'-diaminodiphenylmethane (TGDDM)/ 4,4'-diaminodiphenylsulphone (DADPS) epoxy resin used in aerospace and military applications, is typically brittle and has

a maximum elongation at room temperature of approximately 1.8 % [20]. Hence, a linear elastic approximation may provide a reasonable estimate of the matrix material behavior in the composite, even though the initiation of failure in the composites may involve nonlinear matrix behavior on the microscopic scale. For commercial filament winding applications flexible epoxy resins are often used for impact resistance and greater elongation. These resins may have ultimate elongations of approximately 8 % [21]. In the special case of interfacial shear strength measurements derived from the single fiber fragmentation (SFF) analysis, the epoxy matrix is also required to have a high extension-to-failure, greater than 7 %. This is typically achieved by undercuring the resin [22] or using flexible hardeners to reduce the resin crosslink density [23]. Polymer materials exhibiting high extension-to-failure usually exhibit increased stress relaxation and nonlinear stress-strain behavior in the high strain region. In durability analyses, where the specimen has been exposed to moisture, the stress-strain behavior is often altered by moisture absorption, via plasticization. Hence, the linear elastic matrix assumption may be violated during the fragmentation process.

In this paper, the impact of matrix viscoelasticity on the SFF analysis procedure is investigated. The Cox model is utilized since it explicitly includes the effect of the matrix modulus in the equations for the fiber stress profile, shear stress profile at the fiber matrix interface, and the theoretical critical transfer length. As a first step toward understanding the effect of nonlinear viscoelasticity, we will extend the Cox model to accommodate linear viscoelasticity. Since research on nonlinear constitutive behavior in solids is complicated and still in its infancy, an engineering approximation of the nonlinear stress-strain behavior of the matrix will be presented. The impact of this engineering approximation on the analysis of data obtained from the single fiber fragmentation experiment will be considered.

Theory

The Cox model [2], developed in 1952, is a widely recognized and utilized linear elastic based unit composite model. This model affords the following equations for the stress profile of the embedded fiber, shear stress profile at the fiber-matrix interface, and maximum shear stress for a fiber at its critical length:

$$\sigma_f\{z\} = (E_f - E_m)\epsilon \left[1 - \frac{\cosh\beta\left(\frac{l}{2} - z\right)}{\cosh\beta\frac{l}{2}} \right] \quad (1)$$

$$\tau_{\text{interface}}\{z\} = \frac{d\beta\sigma_c}{4} \left(\frac{E_f - E_m}{E_m} \right) \frac{\sinh\beta\left(\frac{l}{2} - z\right)}{\cosh\beta\frac{l}{2}} \quad (2)$$

$$\tau_{\text{interface}_{\text{max}}}\{l_c\} = \frac{d\beta}{4} \frac{\sinh\beta\left(\frac{l_c}{2}\right)}{\cosh\beta\left(\frac{l_c}{2}\right) - 1} \sigma_f\{l_c\} \quad (3)$$

$$\beta = \frac{2}{d} \left[\frac{E_m}{(1 + \nu_m)(E_f - E_m) \ln\left(\frac{2r_m}{d}\right)} \right]^{\frac{1}{2}} \quad (4)$$

where

$\sigma_f\{z\}$	is the tensile stress in the fiber
$\tau_{interface}\{z\}$	is the shear stress along the fiber-matrix interface
E_f	is the fiber elastic modulus
E_m	is the matrix elastic modulus
l	denotes the length of the fiber
z	is the distance along the fiber
ϵ	is the general or global strain
l_c	is the critical transfer length or ineffective length
σ_c	is the uniform stress applied to the composite
d	is the fiber diameter
r_m	is the radius of the matrix
ν_m	is Poisson's ratio of the matrix

Of notable interest is the quantity β , which has been associated with the critical transfer length of the shear stress transfer process, $l_c/2 \cong 1/\beta$ [7,24]. With respect to the Cox model, β is used in determining the maximum shear stress in the interface (see equation 3) at the critical transfer length. The determination of β has recently come under scrutiny because of its dependence on the nebulous radius of matrix, r_m , parameter (see equation 4) [25-28]. Also of interest is the assumption by Cox, that the maximum stress transferred to the embedded fiber by shear is limited to the difference between the actual displacement at a point on the interface, at a distance "z" from the end of the fiber, and the displacement that would be observed if the fiber were absent. For an E-glass fiber, modulus 67.5 GPa, embedded in an elastic matrix, modulus 2.51 GPa, only 96 % of the matrix shear stress is transferred to the fiber.

Linear Viscoelastic Composite Models.

In 1968-1970, J. M. Lifshitz [29-33] published extensively concerning the effect of linear viscoelasticity on the longitudinal strength of unidirectional fibrous composites. His research focused primarily on investigating the impact of viscoelasticity on composite time dependent fracture or creep rupture. This research was driven by the experimental observation that the longitudinal strength of unidirectional fiber reinforced composites is time dependent. In addition, the elastic based cumulative weakening composite model of Rosen [10,11] assumed fracture in a single cross section of the composite, while experimental evidence showed a very complicated fracture surface. In his research, Lifshitz noted that in many cases of practical importance the matrix material is a polymer having time dependent properties that can be characterized by the laws of linear viscoelasticity. He hypothesized that the existence of breaks in the fibers results in local shear stresses in the matrix that can be expected to relax. Therefore, the length of the fiber fragment required to transmit the load from the matrix to the fiber (ineffective length) increases with time due to the relaxation of the matrix modulus. This sequence of events suggested to Lifshitz the likelihood of a time-dependent failure process for fibrous composites, even for unidirectional composites loaded in the fiber direction. In the development of his viscoelastic model, Lifshitz extended the cumulative weakening model of Rosen [10,11] to the linear viscoelastic regime by utilizing Schapery's Approximation (*Schapery's Correspondence Principle* [34,35]) of the *Elastic-Viscoelastic Correspondence Principle*.3636

$$\sigma_f\{z, t\} = \sigma_{f_0} [1 - \exp(-\eta\{t\}z)] \quad (5)$$

$$\tau_f\{z, t\} = \left(\frac{G_m\{t\}}{2E_f} \frac{r_f}{r_m - r_f} \right)^{1/2} \exp(-\eta\{t\}z) \quad (6)$$

$$\eta\{t\} = \left(\frac{2G_m\{t\}}{E_f} \frac{1}{r_f(r_m - r_f)} \right)^{1/2} \quad (7)$$

$$\delta\{t\} = \left[J_m\{t\} \frac{E_f r_f (r_m - r_f)}{2} \right]^{1/2} \ln \left[\frac{1}{(1 - \Phi)} \right] \quad (8)$$

where

σ_{f_0} is the tensile stress in the fiber at a large distance from the fiber end

In this formulation, Lifshitz chose the ratio $(r_f/r_m)^2$ to be the same value as the volume fraction of the fibers within the composite. Using this approach, a composite with a fiber volume fraction of 40 % and specific gravity of 1.40 has a r_f/r_m value of 0.4 [2]. Assuming the average fiber diameter is 15 μm , r_m has a value of 37.5 μm . In the single fiber fragmentation specimen, the fiber volume fraction is approximately 4×10^{-5} . Hence, r_m is 5.2 mm using this formula. Since the dogbone specimens are approximately 1 mm thick, this has led some to take r_m to be half the specimen thickness [7]. However, this would imply that the interfacial shear strength is dependent on specimen size! Therefore, researchers have focused on ways to accurately determining this parameter.

Equations 5 and 7 show that the stress profile in the fiber is time dependent, via the shear modulus of the matrix, $G_m\{t\}$. In addition, the ineffective length (denoted by $\delta\{t\}$ in this model) is defined as the distance required to transfer the stress from the matrix to the fiber is defined as the ineffective length. The ineffective length is time dependent through the matrix creep compliance, $J_m\{t\}$. From his viscoelastic model Lifshitz, noted that the stress at any point in this zone will relax with time. For a diglycidyl ether of bisphenol-A/bis(2,3-epoxycyclopentyl) ether/aromatic diamine blend system he calculated a relative relaxation of 13 % of the initial stress at infinite time. The ratio of the stress at infinite time to the initial stress is given by Φ in equation 8. To account accurately for the long-term time dependent strength of fibrous composites, Lifshitz suggested that the viscoelastic nature of the glass fibers be considered in addition to the matrix viscoelasticity. Based on his results, Lifshitz viewed the viscoelastic properties of the matrix as the main cause of time dependent strength of fibrous composites.

Making note of Lifshitz's research, Phoenix in 1988 [37] extended his "chain of bundles" model by including the linear viscoelastic effects of the matrix material. To incorporate viscoelastic effects, Phoenix made use of Hedgepeth's solution from the linear elastic case. This solution showed that the geometric load transfer length (ineffective transfer length), δ , varied as $\sqrt{E_f/G_m}$ where E_f is the fiber tensile modulus and G_m is the matrix shear modulus. Harlow and Phoenix showed that the geometric load transfer length, is related to the effective load transfer length, δ^* , and bounded by the following expression:

$$1/(\zeta + 1) \leq \delta^* / \delta \leq 3/(\zeta + 1) \quad (9)$$

Hence, δ^* , with statistical effects included, is considerably shorter than δ and depends on the Weibull shape parameter, ζ , for fiber strength [40]. Phoenix *et al.* [37] quantified the time dependence of δ , resulting from the viscoelasticity of the matrix, by using a power-law creep function

$$J_m\{t\} = J_o \left[1 + (t/t_o)^\theta \right], t \geq 0 \quad (10)$$

where θ and t_o are the creep exponent and time constants, respectively, and $J_o = 1/G_m$.

Although the correlation with experimental data was not perfect, Phoenix's research indicated that the prediction capability of the "chain of bundles" model could be improved by careful characterization of fiber strength, matrix creep, and time-dependent debonding at the fiber-matrix interface. The research by Lifshitz and Phoenix indicates that matrix viscoelastic effects in the creep rupture of unidirectional fibrous composites are important. In addition to these researchers, Jansson and Sundstrom [41] noted that the viscoelastic properties of the matrix play an important role in the creep as well as in the creep rupture processes in composite materials. They indicate that composite matrix materials exhibit *nonlinear anelastic behavior* at low strains and that this behavior becomes pronounced above 1 % strain.

Linear Viscoelastic Cox Model

Even though unit composite analyses, *e.g.*, single fiber fragmentation (SFF) tests, have been used extensively to link microstructural interface research to composite performance, very little research has been done to quantify the impact of matrix viscoelasticity on unit composite analysis methods. One reason for this is that much of the early work assumed that the DGEBA/m-PDA epoxy resin system behaved in an elastic-perfectly plastic manner. Hence, interfacial shear strength values were obtained using the Kelly-Tyson model. This model contains no parameters related to matrix properties and so the inference was that matrix properties were not important.

It should be noted that the SFF test is performed in different ways. Some researchers strain the test specimen at a constant strain rate and continuously monitor and count break events by acoustic emissions (AE) and/or a video camera. The analysis proceeds until the fiber stops breaking with further extension. In principle, viscoelastic effects in this testing regime are exhibited when the strain rate of the test is changed. Therefore, results from tests performed at different strain rates may not be comparable unless the model accounts for changes in matrix properties due to viscoelasticity.

A second approach, utilized in this laboratory, is the manual application of sequential step strains (saw-toothed loading pattern) until saturation is reached. The step strains are made at constant time intervals, usually 10 min, and the number of breaks are counted after each step. The complete distribution of fragment lengths is obtained after saturation is reached. To perform a more detailed analysis of the fragmentation process, *e.g.*, (1) obtain a map of the fragmentation process, (2) obtain fragment lengths at each strain increment, and (3) monitor the development of debond regions during the testing procedure, the time increment between successive strains must be allowed to increase to the time required to measure the fragment lengths after each strain increment. Since the matrix material is viscoelastic

and the stress response of the matrix at a given time, t , depends on the previous stress history, the impact of matrix viscoelasticity on the fragmentation process and the ability to compare results obtained by different testing regimes can become a complex issue.

Because of the similarity between the linear elastic field equations (i.e., equilibrium equation, boundary conditions, strain equations, etc.) and the transform of the linear viscoelastic field equations, Laplace transformed viscoelastic solutions can be obtained from elastic solutions by replacement of the elastic moduli and elastic Poisson's ratio, ν , by the Carson transform of the appropriate viscoelastic relaxation functions and viscoelastic Poisson's ratio (*Elastic-Viscoelastic Correspondence Principle*) [36]. This simple replacement holds if quasi-static and separation of variables, i.e., $\sigma_f\{z, t\} = \bar{\sigma}_f\{z\}g\{t\}$, conditions prevail [42]. The transformed viscoelastic Cox equations are readily written down from equations 1-4. The transformed expressions of equations 1 and 4 are given below:

$$\bar{\sigma}_f\{z, \lambda\} = (E_f - \lambda \bar{E}_m\{\lambda\}) \epsilon \left[1 - \frac{\cosh \bar{\beta}\{\lambda\} (l/2 - z)}{\cosh \bar{\beta}\{\lambda\} l/2} \right] \quad (11)$$

$$\bar{\beta}\{\lambda\} = \frac{2}{d} \left[\frac{\lambda \bar{E}_m\{\lambda\}}{(1 + \lambda \bar{\nu}_m\{\lambda\})(E_f - \lambda \bar{E}_m\{\lambda\}) \ln(2r_m/d)} \right]^{1/2} \quad (12)$$

To transform equation 11 into the time domain $E_m\{\lambda\}$ must be specified analytically. Unfortunately, the inversion of the resulting equation is not trivial. An approximate method of Laplace transform inversion has been given by Schapery, *Schapery's Correspondence Principle: Direct Method* [35]. Schapery notes that if a function $f\{t\}$ has a small curvature when plotted against $\log_{10}t$, the following condition applies:

$$f\{t\} \cong [\lambda \bar{f}\{\lambda\}]_{\lambda=0.5t} \quad (13)$$

The "small curvature" restriction means that when $f\{t\}$ is plotted against $\log_{10}t$ and a tangent is drawn to $f\{t\}$ at any point, the net algebraic area, A_D , enclosed by the tangent line, the function $f\{t\}$, and about three-fourths to one decade on each side of the tangency point should be small relative to the area, A_T , under $f\{t\}$ in the same interval. Schapery indicates that if $f\{t\}$ has constant curvature over a 1.8 decade interval, one can show that the relative error in $f\{t\}$ is essentially equal to the area ratio, A_D/A_T , for this interval.

As a result of the above approximation, Schapery notes that with respect to moduli, a viscoelastic solution is obtained from an elastic solution by replacing all elastic constants with time-dependent relaxation moduli, *Schapery's Correspondence Principle: Quasi-Elastic Method* [35]. In a critique of Schapery's approximations, Christensen indicates that this method is applicable to quasi-static problems in viscoelasticity, for which the deformation history is rather smooth [42].

Krishnamachari [43] notes two additional engineering approximations that may be used to convert the Laplace transformed viscoelastic solutions to the time domain. The first assumes the bulk modulus in the *Elastic-Viscoelastic Correspondence Principle* is constant. This approach is based on the observation that of all the viscoelastic properties, the bulk modulus varies the least with time. Support for this assumption is found in the work of Tschoegl [44] where he notes that in many synthetic polymers the bulk relaxation modulus

changes from the glassy to the equilibrium state by only a factor of about 2 to 3 while the shear modulus changes by 3 to 4 logarithmic decades. The second approach is closely related to Schapery's approximations and is called *pseudoelasticity* [43]. In *pseudoelasticity*, Poisson's ratio, ν , is assumed to be a constant and the elastic moduli are replaced by their viscoelastic counterparts. This approach is based on the observation that ν , although subject to variations of up to (35 to 40) %, is still a weak variable in the expressions for stress and strain, and can be treated as constant in engineering calculations. Christensen [42] indicates that in most quasi-static cases where separation of variables conditions prevail ν is indeed a constant.

Assuming the matrix material meets Schapery's small curvature approximation, the impact of embedding an elastic fiber into a linear viscoelastic matrix is readily seen by utilizing *Schapery's Correspondence Principle* on the Cox model. The linear viscoelastic version (quasi-elastic approximation) of this unit composite model is shown below:

$$\sigma_f\{z, t\} = (E_f - E_m\{t\})\epsilon \left[1 - \frac{\cosh\beta\{t\}\left(\frac{l}{2} - z\right)}{\cosh\beta\{t\} \frac{l}{2}} \right] \quad (14)$$

$$\tau_f\{z, t\} = \frac{d\beta\{t\}\sigma_c}{4} \left(\frac{E_f - E_m\{t\}}{E_m\{t\}} \right) \frac{\sinh\beta\{t\}\left(\frac{l}{2} - z\right)}{\cosh\beta\{t\} \frac{l}{2}} \quad (15)$$

$$\tau_{f_{\max}}\{l_c\{t\}, t\} = \frac{d\beta\{t\}}{4} \frac{\sinh\beta\{t\}\left(\frac{l_c\{t\}}{2}\right)}{\cosh\beta\{t\}\left(\frac{l_c\{t\}}{2}\right) - 1} \sigma_f\{l_c\{t\}\} \quad (16)$$

$$\beta\{t\} = \frac{2}{d} \left[\frac{E_m\{t\}}{(1 + \nu_m\{t\})(E_f - E_m\{t\}) \ln\left(\frac{2r_m}{d}\right)} \right] \quad (17)$$

Because of the time dependence of the viscoelastic matrix, we can see that the critical transfer length, the maximum interfacial shear stress, the shear stress profile of the matrix-fiber interface, and the stress profile in the fiber are time dependent. Equation 16 is of particular interest since its linear elastic counterpart, equation 3, has been used to determine the interfacial shear strength at saturation. As a consequence of the time dependence of the matrix, the linear viscoelastic Cox model indicates that the interfacial shear strength at saturation will depend on what influence the matrix relaxation has on the critical transfer length.

Experimental

Fiber and Mold Preparation

To make single fiber fragmentation specimens eight-cavity molds were made out of RTV-664 (General Electric**) following the procedure described by Drzal [45]. All molds were post cured at 150 °C and rinsed with acetone prior to use. A 12" long tow was cut from a spool of E-glass fibers (from Owens-Corning) previously shown to be bare with no processing aids. The tow was washed with spectrophotometric grade acetone, vacuum dried at 100 °C overnight, and cooled prior to use. Single filaments of E-glass fiber were separated from the 12" tow being careful to touch only the ends of the fiber. The fibers were aligned in the mold cavity via the sprue slots in the center of each cavity. The fibers were temporarily fixed in place by pressing them onto double-stick tape. Small strips of double-stick tape were placed over each fiber end to hold them in place until each fiber was permanently mounted with 5 min epoxy.

Embedding Procedure.

100 grams of diglycidyl ether of bisphenol-A (DGEBA, Epon 828 from Shell Chemical Co.) and 14.5 grams of meta-phenylene diamine (m-PDA, Fluka Chemical Company), were weighed out in separate beakers. To lower the viscosity of the resin and melt the m-PDA crystals, both beakers were placed in a vacuum oven (Fisher Scientific Isotemp Vacuum Oven, model 281 A) set at 75 °C. After the m-PDA crystals were completely melted, the silicone molds containing the fibers were placed into another oven (Blue M Stabiltherm, model OV-560A-2) that is preheated to 100 °C. With the preheated oven turned off, the silicone molds were placed in the oven for approximately 20 min. This last procedure dries the molds and minimizes the formation of air bubbles during the curing process.

At approximately 9 min before the preheated molds were removed from the oven, the m-PDA is poured into the DGEBA and mixed thoroughly. The mixture was placed into the Vacuum Oven and degassed for approximately 7 min. After 20 min, the preheated molds were removed from the oven and filled with the DGEBA/m-PDA resin mixture using 10cc disposable syringes. The filled molds were then placed into a programmable oven (Blue M, General Signal, model MP-256-1, GOP). A cure cycle of 2 h at 75 °C followed by 2 h at 125 °C was used.

Fragmentation Test.

The fiber fragmentation tests were carried out on a small hand operated loading frame similar to that described by Drzal [45] mounted on a Nikon Optiphot polarizing microscope. The image was viewed using a CCD camera (Optronics LX-450 RGB Remote-Head microscope camera) and monitor (Sony, PVM-1344Q). Before the test, the fiber diameter was measured with an optical micrometer (VIA-100 from Boeckeler) attached to the video system. The sample was scanned by translating the loading frame under the microscope with a micrometer. The position of the load frame is monitored by an LVDT (Trans-Tek, Inc.

** Certain commercial materials and equipment are identified in this paper to specify adequately the experimental procedure. In no case does such identification imply recommendation or endorsement by the National Institute of Standards and Technology, nor does it imply necessarily that the product is the best available for the purpose.

model 1002-0012) connected to an A-to-D board (Strawberry Tree, Inc.) in a computer. To measure fragment lengths or other points of interest in the sample, the location was aligned with a cross hair in the microscope as seen on the video monitor, and the position of the LVDT was digitized into the computer. The standard instrument uncertainty in measuring a point is $\pm 0.3 \mu\text{m}$. The standard uncertainty in relocating a point reproducibly is $\pm 1.1 \mu\text{m}$. The load is also monitored during the experiment using a 2,224 N (500 pound) load cell connected to a bridge (load cell and AED 9001A bridge, Cooper Instruments). The expected standard uncertainty of the load measurements is 3 % of the load. The bridge is attached to the same computer via a serial connection. A custom program was developed to continuously record the load and any LVDT measurements that are made. The average application time of each strain step was $(1.10 \pm 0.17) \text{ s}$ and the average deformation was $(14.45 \pm 3.11) \mu\text{m}$. The strain was found to increase by 0.0034 % for each 1 N change in load.

Results and Discussion

Viscoelastic Loading Profile

A typical load-time curve for a DGEBA/m-PDA epoxy resin SFF test specimen is shown in Figure 1 (lower curve). Readily visible in this loading curve is the relaxation of the load after each strain increment. The relaxation of the stress with time is consistent with the constitutive law which governs the behavior of linear viscoelastic materials to step-strain responses, $\sigma\{t\}_{output} = E\{t\}\epsilon_{input}$. The modulus, $E\{t\}$, is the relaxation modulus of the viscoelastic material and is the ratio of the time dependent stress to the initial applied strain. Initially this relaxation modulus has a maximum value, $E_{unrelaxed}$, which corresponds to the instantaneous elastic response. At a time $t \rightarrow \infty$ the modulus attains a minimum value $E_{relaxed}$. This contrasts with the stress response of a linear elastic material to a step strain in-

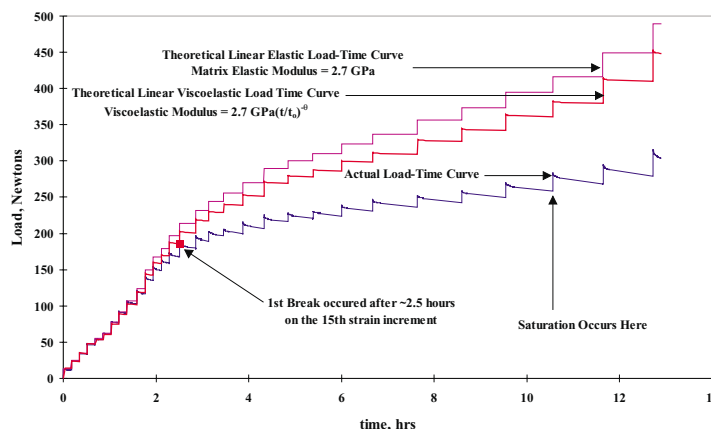


FIG. 1 Actual load-time curve with linear elastic and linear viscoelastic approximations for bare E-glass fiber SFF test specimen.

put, $\sigma_{output} = E_{elastic} \epsilon_{input}$. In such a material the modulus, $E_{elastic}$, is constant with time and so the response to the applied strain is constant with time.

Using the small strain response, $\epsilon < 0.1$, of the actual load-time curve, linear elastic and linear viscoelastic approximations of the load-time curve are also shown in Figure 1. For the linear elastic approximation a modulus value of 2.7 GPa was used. For the linear viscoelastic approximation the time dependent modulus was approximated by a power law expression and Boltzmann's superposition principle [46].

$$E\{t\} = E_o \left(\frac{t}{t_o} \right)^{-\theta} \quad (18)$$

From the step-strain response at small strains, the value of theta, θ , was found to be 0.016 when t_o was taken to be 100 seconds. Good agreement was obtained with the initial strain increments of the saw tooth loading pattern in Figure 1 using both approximations. However, significant deviations arise before the first fiber break occurs, ~ 2.5 h. At saturation, ~ 3.6 % strain, both approximations have deviated considerably from the actual load-time curve. This deviation is indicative of nonlinear stress-strain behavior. Thus fiber fracture is observed in the region where the matrix is exhibiting nonlinear viscoelastic behavior. In this test the time between strain increments is increased after the initial break and increases to the time required to measure the fiber fragments.

Viscoelastic Stress Strain Curves

"Pseudo-isochronal" stress versus strain plots from the data given in Figure 1 are shown in Figure 2. By this term we will mean the clock will be figuratively restarted after each loading step so we can compare loads after each loading step at the same time into that step. For example, the 10 min data will be the load recorded 10 min after each loading step was applied, i.e, the previous peak load [39,41]. Figure 2 shows data at 10 s (10 s stress) and 10 min (10 min stress) for the sample shown in Figure 1. Since the time increment between step-strains varied, the stress immediately before the application of the next strain increment is also plotted. The measurement of fragment lengths began at 10 min after the step-strain was applied. Consequently, the separation between the 10 min stress plot and the stress before the next strain increment plot indicates the degree of stress relaxation and hence, matrix relaxation occurring during the measurement of the fragment lengths. In Figure 2 the 10 s stress values from the theoretical linear viscoelastic fit in Figure 1 are depicted by open circles. As expected the linear viscoelastic fit is intermediate between the linear elastic fit and the 10 stress-strain data in the high strain region. From Figure 2 it is clear that for the specific loading history in this experiment, the epoxy matrix exhibits nonlinear stress-strain behavior above 1 % strain. Regression analyses of the data below 1 % strain and above 1.8 % strain shows that the *tangent moduli* for the 10 s stress data are (2.52 ± 0.01) GPa and (1.15 ± 0.01) GPa, respectively (see Figure 2). Regression analyses of the 10 min stress-strain data resulted in *tangent moduli* values of (2.46 ± 0.01) GPa and (1.11 ± 0.01) GPa, respectively. However, the *tangent moduli* in the region above 1.8 % strain are significantly less, ~ 55 %, than the *tangent moduli* in the small strain region.

Based on these observations, a linear analysis of the interfacial shear stress via the Cox model, utilizing the small strain "linear elastic" modulus of the viscoelastic matrix, is not appropriate. From related research, numerical simulations of the fragmentation process using a linear elastic matrix results in an over prediction of the number of fragments that actually occur [47]. In addition, the onset of fragmentation in the unit composite specimens investi-

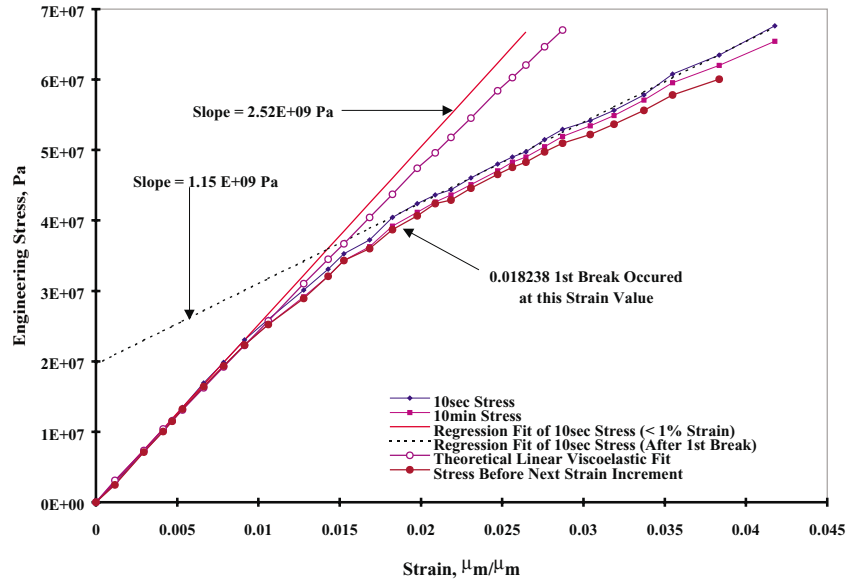


FIG 2. Pseudo-isochronal stress-strain plots for SFF test specimen containing a bare E-glass fiber (variable loading time increments).

gated by Feillard *et al* [47] occurred in the nonlinear stress strain region, $\sim 5\%$ strain. Since the epoxy matrix exhibits increased load carrying capability after the onset of yield, the Kelly-Tyson model which assumes an elastic perfectly plastic matrix material is also a poor approximation.

Nonlinear Viscoelastic Model

Since the onset of fiber fracture occurs in the nonlinear stress-strain region, existing shear lag unit composite models must be extended to account for the nonlinear viscoelastic constitutive behavior of the matrix. Unfortunately, the development of nonlinear constitutive equations and models for solids is a complicated and active area of research. At present there is no universal theory for developing nonlinear constitutive equations for melts or solids and, hence, all nonlinear models are somewhat empirical in nature. Motivated by the fact that matrix properties in the Cox and linear viscoelastic Cox model arise primarily through the matrix modulus and Poisson's ratio, it is plausible to assume that strain dependent nonlinear effects involving the matrix are also manifested in these terms. Accepting this general format, one can make the engineering approximation that Poisson's ratio is a constant and replace the relaxation modulus, $E_m\{\epsilon, t\}$, in the linear viscoelastic Cox model with a modulus dependent on strain and time, $E_m\{\epsilon, t\}$. Thus, the nonlinear viscoelastic Cox equations have the following functional forms and variable dependencies:

$$\sigma_f\{z, \varepsilon, t\} = (E_f - E_m\{\varepsilon, t\})\varepsilon \left[1 - \frac{\cosh\beta\{\varepsilon, t\}\left(\frac{l}{2} - z\right)}{\cosh\beta\{\varepsilon, t\} \frac{l}{2}} \right] \quad (19)$$

$$\tau_f\{z, \varepsilon, t\} = \frac{d\beta\{\varepsilon, t\}\sigma_c}{4} \left(\frac{E_f - E_m\{\varepsilon, t\}}{E_m\{\varepsilon, t\}} \right) \frac{\sinh\beta\{\varepsilon, t\}\left(\frac{l}{2} - z\right)}{\cosh\beta\{\varepsilon, t\} \frac{l}{2}} \quad (20)$$

$$\tau_{f_{\max}}\{l_c, \varepsilon, t\} = \frac{d\beta\{\varepsilon, t\}}{4} \frac{\sinh\beta\{\varepsilon, t\}\left(\frac{l_c}{2}\right)}{\cosh\beta\{\varepsilon, t\}\left(\frac{l_c}{2}\right) - 1} \sigma_f\{l_c\} \quad (21)$$

$$\beta\{\varepsilon, t\} = \frac{2}{d} \left[\frac{E_m\{\varepsilon, t\}}{(1 + \nu_m)(E_f - E_m\{\varepsilon, t\}) \ln\left(\frac{2r_m}{d}\right)} \right] \quad (22)$$

A plot of the relaxation modulus versus $\ln(t)$, Figure 3, indicates that Schapery's small curvature approximation is met well into the nonlinear stress-strain region. The development of a

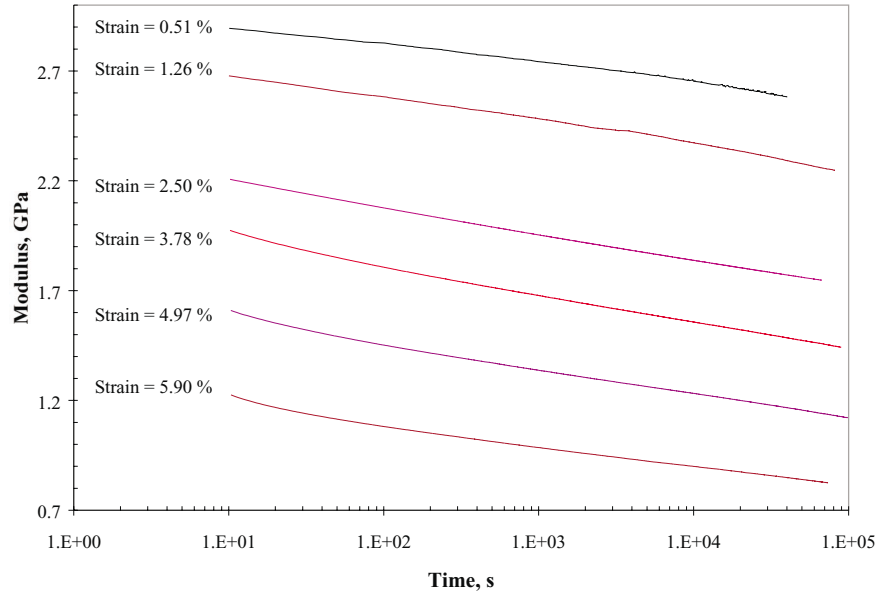


FIG 3. Single-step relaxation behavior of DGEBA/m-PDA dogbone specimens.

nonlinear viscoelastic relaxation modulus will be the subject of future work. In the absence of an explicit expression for $E_m\{\epsilon, t\}$, the matrix nonlinearity is further approximated by substituting into the nonlinear viscoelastic Cox model a “secant modulus”, or average modulus, which is dependent on strain and time. In the nonlinear stress-strain region this modulus is readily calculated from the experimental stress-strain data at each strain increment. This modulus should provide a conservative estimate of the impact of nonlinear viscoelasticity on the SFF test. Therefore, in the above equations

$$E_m\{\epsilon, t\} = \langle E_m\{\epsilon, t\} \rangle_{secant} \quad (23)$$

Additional, motivation for the use of a strain dependent secant modulus is found in the work of Feillard *et al* [47] As noted previously, numerical simulations of the single fiber fragmentation process using a linear elastic matrix overpredicted the number of fragments that actually occur. These researchers found better agreement using a secant modulus.

Impact of Nonlinear Viscoelasticity on the Critical Transfer Length

From the research of Asloun *et al.* [7] the theoretical critical transfer length is given by the following expression:

$$\frac{l_c}{2} \cong \frac{1}{\beta} = \frac{d}{2} \left[\frac{(1 + \nu_m)(E_f - E_m)}{E_m} \ln \left(\frac{2r_m}{d} \right) \right]^{1/2} \quad (24)$$

By replacing E_m in equation 24 with equation 23, the critical transfer length in a nonlinear viscoelastic material becomes time and strain dependent through the matrix modulus. The variation of the secant moduli, nonlinear and linear, with strain and the number of fiber breaks are shown in Figure 4. At the final strain increment the 10 s nonlinear secant modulus has decreased by 35 % relative to the elastic modulus, whereas the linear viscoelastic secant modulus is predicted to decrease by only 6.5 %. Assuming r_m to be 1/2 the thickness of the sample, the impact of these moduli variations on the critical transfer length are shown in Figure 5. Except for the critical transfer length values determined by the theoretical equation of Asloun *et al.* (equation 24), all transfer length values were determined graphically, at 96.5 % of the maximum fiber stress, by substituting the appropriate viscoelastic secant moduli into equations 14 and 19.

Comparing the 10 s nonlinear secant modulus transfer length determined graphically, solid triangles, and transfer length determined theoretically from Asloun’s equation extended to the nonlinear viscoelastic regime, solid circles, indicates that Asloun’s equation captures the relative change in transfer length over the complete strain range, but is off by a constant factor of 1.684. Consistent with the moduli variations shown in Figure 4, the transfer length for the 10 s nonlinear secant modulus at the last strain increment shows an increase of 25 % relative to the elastic transfer length, $l_c/2 = 255 \mu\text{m}$. The transfer length of the linear viscoelastic secant modulus increases by only 3.6 % over the same range. Analysis of the relaxation behavior within a strain step reveals that the relaxation of the secant modulus after 10 min into the strain step increases the transfer length by approximately 2 %. Relaxation of the secant modulus up to 1 h increases the transfer length by less than 5 % in each strain step. These results indicate that the variation in the transfer length from the experimental data is due primarily to the nonlinear behavior of the matrix material in the high strain region.

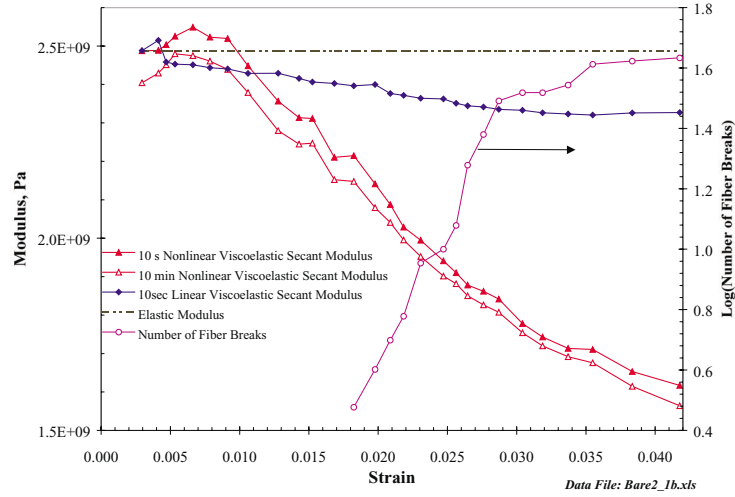


Figure 4. Variation of moduli with strain and number of fiber breaks.

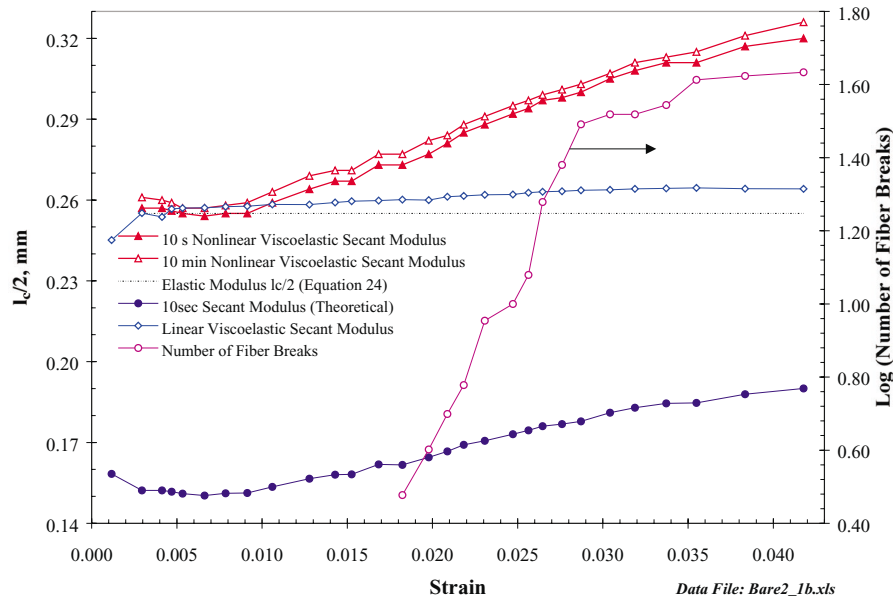


FIG 5. Variation of critical transfer length with strain and number of fiber breaks

Impact of Nonlinear Viscoelasticity on Interfacial Shear Strength Measurements

To determine the interfacial shear strength from the Cox model and its time and strain dependent variants (see equations 3,16, and 21), the critical transfer length (l_c), the value of b , and the stress in the fiber at the critical transfer length ($\sigma_f\{l_c\}$) must be determined. Although the critical transfer length is obtained experimentally, the latter variables must be calculated. The stress at the critical transfer length is typically determined from Weibull parameters and is beyond the scope of this paper. However, Schultheisz *et al.* [48] have reported values for the stress in the fiber at the critical transfer length in the range of (2.5 to 2.8) GPa for fragments similar in size to those generated in this paper. Since this value is not essential for comparing the impact of nonlinear viscoelasticity on the analysis procedure, the value of 2.5 GPa will be used.

Although β is not constant for the viscoelastic models, the value of the matrix modulus at saturation is used to calculate β and determine the interfacial shear strength for all models. The use of this modulus value in the viscoelastic model is motivated by our desire to carry out durability analysis. Since the fiber strength has been shown to decrease with exposure to moisture, it is desirable to calculate the fiber strength value from the test data. Since the procedure devised by Schultheisz *et al.* [48] calculates the fiber strength at saturation, the value of the secant modulus at this value is appropriate. Recognizing that the secant modulus at saturation is dependent on the previous deformation history, the following guidelines were followed to minimize test variability in the measured secant modulus. (1) Multi-step loading was kept uniform, i.e., step-strains were nominally the same throughout the experiment with no premature unloads of the matrix. (2) The variability in intersample loading profiles was minimized. Intersample changes were limited to normal changes that are incurred from measuring or counting the fragments after each strain step. (3) The profile of the fragment distributions at the end of the test was checked in each sample and found to be nominally the same. (4) The incubation time, i.e., time before fragments are counted or measured, remained the same. For the DGEBA/m-PDA epoxy resin this time was 10 min.

In Table 1 the determined interfacial shear strength using the various moduli are shown. When the nonlinear secant modulus is used the determined interfacial shear strength is 20 % lower than the value obtained when the elastic modulus value that is typically assumed for the DGEBA/m-PDA epoxy resin is used. The interfacial shear strength obtained by using the elastic modulus derived from the experimental data lowers the interfacial shear strength by approximately 8 %. As expected from the data depicting the variation in moduli with strain (see Figure 4), the interfacial shear strength obtained from the linear viscoelastic secant modulus is approximately the same as the value obtained from the experimental data

Table 1 - *Determined interfacial shear strength using various moduli.*

	Modulus, GPa	β , mm ⁻¹	τ , MPa
Elastic Modulus, Assumed	3.06	14.48	116
Elastic Modulus, via Experimental Data	2.52	13.09	107
Linear Viscoelastic Secant Modulus	2.32	12.54	104
Nonlinear Secant Modulus	1.71	10.7	93
Kelly-Tyson Model	N/A	N/A	30

elastic modulus. Utilizing the experimentally determined critical transfer length of 502 μm and the fiber diameter of 12.12 μm , the Kelly-Tyson model which has been widely used to analyze glass fibers embedded in this resin yields an interfacial shear strength value 3 to 4 times smaller than the elastic and secant moduli estimates.

Conclusions

Experimental data was presented for a single fiber fragmentation test specimen consisting of a bare E-glass fiber embedded in DGEBA/m-PDA epoxy resin. The data conclusively showed that fragmentation in the E-glass fiber occurred in the nonlinear viscoelastic region of the stress strain curve. In addition, the DGEBA/m-PDA epoxy resin was shown to exhibit increased load carrying capability after the onset of yield. Hence, the linear elastic Cox model and the Kelly-Tyson model were shown to be inappropriate for analyzing fragmentation data from this test specimen.

To accommodate the nonlinear viscoelastic behavior of the DGEBA/m-PDA resin, the Cox Equation was first extended to the linear viscoelastic regime by using *Schapery's Correspondence Principle*. Analysis of the DGEBA/m-PDA epoxy resin step-strain data revealed that the criteria for applying *Schapery's Correspondence Principle* was met even in the nonlinear viscoelastic region. Extending the linear elastic Cox model to the viscoelastic regime was shown to result in time dependent expressions for the fiber stress, shear stress, maximum fiber stress, and the parameter β , which has been associated with the critical transfer length. The nonlinear behavior of the matrix material had a major influence on the resulting transfer length.

The nonlinear viscoelastic Cox model was assumed to have a form analogous to the linear viscoelastic Cox model with the time dependent modulus and Poisson's ratio replaced by its time and strain dependent counterparts. In lieu of an explicit expression for the strain dependent modulus and motivated by a desire to do durability analyses, the secant modulus at saturation was chosen as an appropriate modulus to utilize in the nonlinear Cox model. In addition, ν was assumed to be constant. With this approximation, the nonlinear behavior of the matrix was found to contribute significantly to the increase in the transfer length due to its dependence on the modulus. The modulus was found to decrease relative to the small strain modulus by approximately 55 % during the experiment. This decrease in the modulus resulted in a 25 % increase in the critical transfer length relative to the initial value during the experiment. As a result the interface strength calculated by the secant modulus at saturation was found to be 20 % lower than the interface strength predicted by the elastic modulus. As noted previously, numerical simulations of the fragmentation process by Feillard *et al.* [47], assuming a linear elastic matrix was shown to over predict the degree of fragmentation in the specimen. These researchers found better agreement with the use of a "secant modulus". The Kelly-Tyson model which has been widely used to analyze glass fibers embedded in this resin yields an interfacial shear strength value 3 to 4 times smaller than the elastic and secant moduli estimates.

During the review process, it was observed that we have not addressed the impact of the change in fiber tensile strength as a function of fiber length on the determination of the interface strength. As pointed out by one reviewer, this effect will have a larger affect on the determined interfacial shear strength than changes in the matrix modulus and will make the values given in Table 1 much larger than the values that have been determined from measurements made on high volume fraction composites. The reviewer also noted that the number of fragments at saturation is experimentally determined and is relatively independent of the assumptions about matrix material behavior when slow straining rates are used. To the re-

viewer's first comment we noted that no one has effectively dealt with the issue of change in fiber tensile strength as a function of fiber length and this issue remains an active research topic. Over the years, this issue has been discussed at length in our laboratory and because of its complexity, we decided that it should be dealt with as a separate topic. Hence, the values in Table 1 are not absolute values, but are given to illustrate only the effect of modulus changes on the derived value of the interfacial shear strength.

The driving force for the development of the nonlinear viscoelastic model has been the observation that the number of fragments at saturation from E-glass/DGEBA/m-PDA SFFT specimens depends on how the test is performed (test protocol). This observation is inconsistent with the assumption of elastic or elastic-perfectly plastic matrix behavior. Indeed, the reviewer's second observation alludes to this problem. The test protocol issue has also been of central concern in the development of a new round robin test procedure being administered by the Versailles Project on Advanced Materials and Standards (VAMAS). In the proposed VAMAS round robin test procedure, the DGEBA/m-PDA matrix is also used. Ongoing research in this laboratory has shown that the nonlinear viscoelastic model developed in this paper is useful in detecting differences in the fragmentation behavior of E-glass/DGEBA/m-PDA test specimens arising from changes in the test protocol. Since these observations require a detailed discussion of the fragmentation length distributions at saturation, future publications will cover the investigation of the effect of test protocol on the fragment length distribution at saturation and the application of the nonlinear viscoelastic model developed in this paper to this observed fragmentation behavior.

References

- 1 Galiotis, C., Young, R. J., Yenug, P. H. J., Batchelder, D. N., "The Study of Model Polydiacetylene/Epoxy Composites", *Journal of Materials Science*, 19, 1984, 3640-3648.
- 2 Cox, H. L., "The Elasticity and Strength of Paper and Other Fibrous Materials", *British Journal of Applied Physics*, 3, 1952, 72-79.
- 3 Melanitis, N., Galiotis, C., Tetlow, P. L., Davies, C. K. L., "Interfacial Shear Stress Distribution in Model Composites Part 2: Fragmentation Studies on Carbon Fibre/Epoxy Systems", *Journal of Composite Materials*, 26(4), 1992, 574-610.
- 4 Kelly, A., Tyson, W. R., "Tensile Properties of Fibre-Reinforced Metals: Copper/Tungsten and Copper/Molybdenum", *Journal of Mechanics and Physics of Solids*, 13, 1965, 329-350.
- 5 Kelly, A., Tyson, W. R., "Fiber-Strengthened Materials", in *High Strength Materials: Proceedings of the 2nd. Berkeley International Materials Conference*, Ed. V. F. Zackay, John Wiley & Sons, Inc.: New York (1964), Chapter 13.
- 6 Kelly, A., "The Strengthening of Metals by Dispersed Particles", *Proceedings of the Royal Society of London*, A282, 63-79.
- 7 Asloun, EI. M., Nardin, M., Schultz, J., "Stress Transfer in Single-Fibre Composites: Effect of Adhesion, Elastic Modulus of Fibre and Matrix, and Polymer Chain Mobility", *Journal of Materials Science*, 24, 1989, 1835-1844.
- 8 Shioya, M., McDonough, W. G., Schutte, C. L., Hunston, D. L., "Test Procedure for Durability Studies of the Fiber Matrix Interface", in the *Proceeding so the Seventeenth Annual Meeting and the Symposium on Particle Adhesion*, ed. K. M. Liechti, The Adhesion Society: Orlando, Fl., 1994, 248-251.
- 9 Dow, N. F., "Study of Stresses Near a Discontinuity in a Filament-Reinforced Composite Metal", Report No. R63SD61, General Electric Space Sciences Laboratory (August 1963).
- 10 Rosen, B. W., "Tensile Failure of Fibrous Composites", *American Institute of Aeronautics and Astronautics Journal*, 2(11), 1964, 1985-1991.

- 11 Rosen, B. W., "Mechanics of Composite Strengthening", in *Fiber Composite Materials*, Ed. S. H. Bush, American Society for Metals, Metals Park, Ohio (1965), Chapter 3.
- 12 Amirbayat, J., Hearle, J. W. S., "Properties of Unit Composites as Determined by the Properties of the Interface. Part I: Mechanism of Matrix-Fibre Load Transfer", *Fibre Science and Technology*, 2, 1969, 123-141.
- 13 Amirbayat, J., Hearle, J. W. S., "Properties of Unit Composites as Determined by the Properties of the Interface. Part II: Effect of Fibre Length and Slippage on the Modulus of Unit Composites", *Fibre Science and Technology*, 2, 1969, 143-153.
- 14 Amirbayat, J., Hearle, J. W. S., "Properties of Unit Composites as Determined by the Properties of the Interface. Part III: Experimental Study of Unit Composites Without a Perfect Bond Between the Phases", *Fibre Science and Technology*, 2, 1969, 223-239.
- 15 Smith, G. E., Spencer, A. J. M., "Interfacial Traction in a Fibre-Reinforced Elastic Composite Material", *Journal of the Mechanics and Physics of Solids*, 18, 1970, 81-100.
- 16 Theocaris, P. S., Papanicolaou, G. C., "The Effect of the Boundary Interphase on the Thermomechanical Behaviour of Composites Reinforced with Short Fibres", *Fiber Science and Technology*, 12(6), 1979, 421-433.
- 17 Whitney, J. M., Drzal, L. T., "Axisymmetric Stress Distribution Around an Isolated Fiber Fragment", in *Toughened Composites ASTM STP 937*, Johnson, N.J., ed; ASTM, Philadelphia, Pa (1987).
- 18 McCartney, L. N., "New Theoretical Model of Stress Transfer Between Fiber and Matrix in a Uniaxially Fiber-Reinforced Composite", *Proceedings of the Royal Society of London*, A425, 1989, 215-244.
- 19 Nairn, J. A., "A Variational Mechanics Analysis of the Stresses Around Breaks in Embedded Fibers", *Mechanics of Materials*, 13(2), 1992, 131-154.
- 20 Puglisi, J. S., Chaudhari, M. A., "Epoxy(EP)", in *Engineered Materials Handbook*, Vol. 2, Metals Park, OH. (1988), pp. 240-241.
- 21 Shibley, A. M., "Filament Winding", in *Handbook of Composites*, Ed. G. Lubin, Van Nostrand Reinhold Company (1982), pp. 449-478.
- 22 Drzal, L. T., Rich, M. J., Lloyd, P. A., "Adhesion of Graphite Fibers to Epoxy Matrices: 1. The Role of Fiber Surface Treatment", *Journal of Adhesion*, 16(1), 1982, 1-30.
- 23 Netravali, A. N., Henstenburg, R. B., Phoenix, S. L., Schwartz, P., "Interfacial Shear Strength Studies Using the Single-Filament-Composite Test. 1: Experiments on Graphite Fibers in Epoxy", *Polymer Composites*, 10(4), 1989, 226-241.
- 24 Galiotis, C., Young, R. J., Yeung, P. H. J., Batchelder, D. N., "The Study of Model Polydiacetylene/Epoxy Composites. Part I. The Axial Strain in the Fibre", *Journal of Materials Science*, 19(11), 1984, 3640-3648.
- 25 Melanitis, N., Galiotis, C., Tetlow, P. L., Davies, C. K. L., "Interfacial Shear Stress Distribution in Model Composites: The Effect of Fiber Modulus", *Composites*, 24(6), 1993, 459-466.
- 26 Galiotis, C., "Interfacial Studies on Model Composites by Laser Raman Spectroscopy", *Composites Science and Technology*, 42, 1991, 125-150.
- 27 Melanitis, N., Galiotis, C., Tetlow, P. L., Davies, C. K. L., "Monitoring the Micromechanics of Reinforcement in Carbon Fibre/Epoxy Resin Systems", *Journal of Materials Science*, 28(6), 1993, 1648-1654.
- 28 Li, Zong-Fu, Grubb, D. T., "Single Fiber Polymer Composites. Part 1. Interfacial Shear Strength and Stress Distribution in the Pull-Out Test", *Journal of Materials Science*, 29(1), 1994, 189-202.
- 29 Lifshitz, J. M., "Time Dependent Fracture of Fibrous Composites", in *Composite Materials*. Vol. 5: Fracture and Fatigue, Ed. L. J. Broutman, Academic Press: New York, 1974, Chapter 6.
- 30 Lifshitz, J. M., Rotem, A., "Time-Dependent Longitudinal Strength of Unidirectional Fibrous Composites", *Fibre Science and Technology*, 3(1), 1970, 1-20.
- 31 Lifshitz, J. M., Rotem, A., "An Observation on the Strength of Unidirectional Fibrous Composites", *Journal of Composite Materials*, 4(1), 1970, 133-134.

- 32 Lifshitz, J. M., "Specimen Preparation and Preliminary Results in the Study of Mechanical Properties of Fiber Reinforced Material. Part I", **AFML-TR-69-89**, Air Force Materials Laboratory, Wright-Patterson Air Force Base, Ohio, July 1969.
- 33 Lifshitz, J. M., Rotem, A., "Longitudinal Strength of Unidirectional Fibrous Composites", **AFML-TR-70-194**, Air Force Materials Laboratory, Wright-Patterson Air Force Base, Ohio, September 1970.
- 34 Schapery, R. A., "Approximate Methods of Transform Inversion for Viscoelastic Stress Analysis", *Proceedings of the 4th U.S. National Congress of Applied Mechanics*, ASME (1962), 1075.
- 35 Schapery, R. A., "Stress Analysis of Viscoelastic Composite Materials", *Journal of Composite Materials*, 1(3), 1967, 228-267.
- 36 Lee, E. H., "Stress Analysis in Visco-Elastic Bodies", *Quarterly of Applied Mathematics*, 13(2), 1955, 183-190.
- 37 Phoenix, S. L., Schwartz, P., Robinson IV, H. H., "Statistics for the Strength and Lifetime in Creep-Rupture of Model Carbon/Epoxy Composites", *Composites Science and Technology*, 32, 1988, 81-120.
- 38 Hedgepeth, J. M., "Stress Concentrations in Filamentary Structures", **NASA TN D-882**, Langley Research Center, 1961.
- 39 Harlow, D.G., Phoenix, S. L., "Bounds on the Probability of Failure of Composite Materials", *International Journal of Fracture*, 5(4), 1979, 321-336.
- 40 **Note:** The symbols have been changed in this article (see reference 37) to be consistent with previously referenced research results. Hence, δ denotes the geometric load (ineffective) transfer length and represents the distance along the broken fiber (counting both sides) where the stress is reduced below the maximum stress. δ^* denotes the "effective load transfer length" and represents the length of a fiber segment, *i.e.*, fiber adjacent to the broken fiber, under a constant or uniform stress which would have the same probability of failure as a segment loaded under the assumed triangular overload load profile.
- 41 Jansson, J.-F., Sundstrom, H., "Creep and Fracture Initiation in Fiber Reinforced Plastics", in *Failure of Plastics*, eds. W. Brostow & R. D. Corneliussen, Hanser Publishers: Munich, 1986, Chapter 24.
- 42 Christensen, R. M., "Theory of Viscoelasticity: An Introduction", Academic Press: New York, 1982, Chapter II.
- 43 Krishnamachari, S. I., "Applied Stress Analysis of Plastics: A Mechanical Engineering Approach", Van Nostrand Reinhold: New York, 1993, Chapter 5.
- 44 Tschoegl, N. W., "The Phenomenological Theory of Linear Viscoelastic Behavior", Springer-Verlag: Berlin, 1989, Chapter 11.3.5.
- 45 Drzal, L. T., Herrera-Franco, P. J., "Composite Fiber-Matrix Bond Tests", *Engineered Materials Handbook: Adhesive and Sealants, Vol. 3*, ASM International, Metals Park, Ohio (1990), 391-405.
- 46 Dealy, J. M., Wissbrun, K. F., *Melt Rheology and its Role in Plastics Processing: Theory and Applications*, Van Nostrand Reinhold, New York (1990), pp. 128,132,146,188.
- 47 Feillard, P., Desarmot, G., Favre, J. P., "A Critical Assessment of the Fragmentation Test for Glass/Epoxy Systems", *Composites Science and Technology*, 49, 1993, 109-119.
- 48 Schultheisz, C. R., McDonough, W. G., Kondagunta, S., Schutte, C. L., Macturk, K. S., McAuliffe, M., Hunston, D. L., "Effect of Moisture on E-Glass/Epoxy Interfacial and Fiber Strengths", *Composite Materials: Testing and Design*, ASTM STP 1242.